Large Eddy Simulation using One-Equation SGS Model based on Dynamic Procedure for Flows in Laminar-Transition Region

Open Access

Firdaus Mohamad[1,2,*], Takeo Kajishima[1]

1 Department of Mechanical Engineering, Osaka University 2-1 Yamadaoka, Suita, Osaka 565-0871, Japan
2 Faculty of Mechanical Engineering, Universiti Teknologi MARA (UiTM), 40450 Shah Alam, Selangor, Malaysia

ARTICLE INFO	ABSTRACT
	Prediction of laminar-transition flows around an airfoil remain an issue in the large eddy simulation (LES) community. Hence, this paper aims to solve this issue by introducing a new dynamic one-equation k_{SGS} model (OD). This model uses the advantage of the dynamic Smagorinsky procedure to represent the energy transfer between grid-scale (GS) and sub-grid-scale (SGS). This procedure is incorporated in order to calculate the coefficient in the production term of the turbulent kinetic energy, k_{SGS} transport equation. The dynamic procedure implemented in this work does not require any averaging in homogeneous direction and this has given the OD model an extra advantage in terms of the applicability for engineering applications. The main feature of the OD model has been proven in identifying the non-turbulent region around the airfoil where the k_{SGS} and eddy viscosity automatically turns to zero. In addition, the OD model also has the capability to capture the laminar region even though the grid used is considered coarse. As a result, we revealed that the artificial procedures to vanish the eddy viscosity in laminar region can be resolved by applying the OD model. Thus, the OD model is believed suitable for unsteady flow simulation such as dynamic stall where the transition point is changed with the variation of angle-of-attack.

1. Introduction

Flow around A-profile airfoil (A-airfoil) at angle of attack 13.3° and Reynolds number based on chord length and freestream velocity Re_c=2.1 × 10⁶ has been used as a case study in this paper. The geometry of A-airfoil is shown in Figure 1. Established experimental results from an ONERA wind tunnel revealed a complex flow configuration which involved the laminar-transition region, reattachment and trailing edge separation. These flow configurations have been studied extensively via large eddy simulations (LES) by a group of researchers in a LESFOIL project [1]. Their study was focused on different types of grid arrangements, numerical approach and effect of SGS models.

---

* Corresponding author.
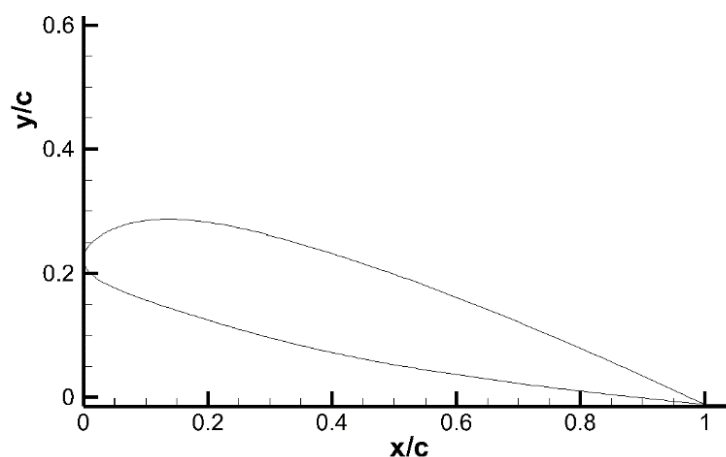*E-mail address: firdausmohamad@uitm.edu.my (Firdaus Mohamad)*

Fig. 1. A-airfoil geometry

Complex flow phenomena over the A-airfoil have offered different complexities to resolve all the important flow structures in large eddy simulations (LES). Both grid arrangement and SGS models play important roles in capturing the flow structures. Mary and Sagaut [2] revealed in their LESFOIL report about the importance of fine grid resolution for the better solution accuracy of pressure coefficient compared to that obtained from the SGS models. On the other hand, they also concluded that the explicit SGS model manages to capture the important flow structures if the grid is sufficiently fine [2]. Even though work from Mary and Sagaut was remarked as the most successful result in a LESFOIL project, their grid arrangement method on the region of flow interest maybe not be a universal method. In 2018, Asada and Kawai revisited the LESFOIL project and their results, with more than 1200 million of nodes, displayed a very good similarity with experimental data [3].

As far as engineering applications are concerned, billions of grid numbers over the flow of interest is not a practical approach to be applied despite the great success by Asada and Kawai [3]. Their method also needed prior information about the flow configuration such as transition and separation point, which in turn is not a universal approach if that information is not on hand. Dahlstrom and Davidson [4] applied a numerical treatment for the laminar and transition region where a bounded second-order upwind scheme was used to remove the unphysical oscillations around the leading edge. Treatment of SGS model was also implemented in the upstream of the transition region where the subgrid scale kinetic energy k_{SGS} was set to zero. Despite of all these treatments, the results in terms of transition point were still far downstream and upstream of the exact transition point [4]. Later, they improved the grid resolution in streamwise direction and as a result, there was SGS dissipation in the laminar region even though a similar treatment was applied [5].

Dynamic procedure is known as an effective method to determine the coefficient locally for large eddy simulation (LES). This procedure was first proposed by Germano *et al.,* [6] and later improved by Lilly [7] to solve the drawbacks of constant eddy viscosity coefficient in the Smagorinsky Model (SM). Later, the dynamic procedure had also been incorporated to determine the coefficient in the transport equation of k_{SGS}. Ghosal *et al.*, [8] stressed the importance of tracing the energy in subgrid scale which allowed for transfer of energy from subgrid scale to resolve scale or energy backscatter. They allowed for negative sign of coefficient calculated through the transport equation of subgrid scale kinetic energy and made the eddy viscosity depend on the subgrid scale kinetic energy k_{SGS}.

In this paper, we aim to remove the artificial treatments in the laminar-transition region by extending the one-equation Dynamic Model (OD) proposed by Kajishima and Nomachi [9]. We believed that the effect of turbulent kinetic energy transfer from GS to SGS was best defined through the production term of k_{SGS} transport equation. This model is different from others in terms of defining the production term. Previous work on dynamic one-equation models defined the

production term based on the eddy viscosity equation which accounted for the square root of k_{SGS}. Taghinia and Rahman [10,11] also calculated the production term in similar approach in their proposed SGS RAST model. However, Inagaki and Abe [12] stressed that the proportion between the production term and square root of k_{SGS} will cause the k_{SGS} to self-reproduce and as a consequence, this procedure is not feasible for non-turbulent regions. An article from Davidson [13] also supported this argument. Meanwhile the OD model defined the production term through the Smagorinsky Model (SM). This procedure performs better in the sense of the non-turbulent region, where the k_{SGS} and v_t become zero. In the OD model, the backscatter is represented by negative production term in k_{SGS} transport equation which in turn can decrease the value of k_{SGS}. However, this backscatter is not represented in filtered equation of motion due to the physical of eddy viscosity v_t that not allow for negative values.

2. Governing Equations
2.1 Basic Equation for LES and the OD Model

Our simulations were based on the incompressible Navier-Stokes equations where all the variables were non-dimensionalized by the chord length C, and the freestream velocity U_∞. Low pass filtering based on spatial filter is used to differentiate between resolvable scale (large) and unresolvable scale (small). The filtering operation is represented as

$$\bar{f}(x) = \int_{-\infty}^{\infty} G(y)f(x-y)\,dy, \tag{1}$$

where G is the "grid filter" function having the representative length corresponding to the width of computational grid. The filtered continuity and momentum equations are

$$\frac{\partial \bar{u}_i}{\partial x_i} = 0, \tag{2}$$

$$\frac{\partial \bar{u}_i}{\partial t} + \frac{\partial}{\partial x_j}\left(\overline{u_i u_j}\right) = -\frac{1}{\rho}\frac{\partial \bar{p}}{\partial x_i} + \frac{\partial}{\partial x_j}\left(2v\bar{D}_{ij}\right) \tag{3}$$

Eq. (3) contains non-linear term $\left(\overline{u_i u_j}\right)$ which cannot be resolved by the grid scale variables. Hence, rewriting the Eq. (3)

$$\frac{\partial \bar{u}_i}{\partial t} + \frac{\partial}{\partial x_j}\left(\bar{u}_i \bar{u}_j\right) = -\frac{1}{\rho}\frac{\partial \bar{P}}{\partial x_i} + \frac{\partial}{\partial x_j}\left[2v\bar{D}_{ij} - \tau_{ij}\right], \tag{4}$$

where $\bar{D}_{ij}$ is the grid-scale rate-of-strain tensor

$$\bar{D}_{ij} = \frac{1}{2}\left(\frac{\partial \bar{u}_i}{\partial x_j} + \frac{\partial \bar{u}_j}{\partial x_i}\right). \tag{5}$$

Eq. (4) consists of $\bar{u}_i$ which is denoted as the GS component of velocity, $\bar{p}(\bar{P} = \frac{\bar{p}}{\rho})$ the GS component of pressure divided by the fluid density ρ and v the kinematic viscosity of fluid. Term τ_{ij} is known as the residual stress or sub-grid-scale stress (SGS) stress. This term consists of unresolved stress which needs to be modelled.

$$\tau_{ij} = \overline{u_i u_j} - \bar{u}_i \bar{u}_j \tag{6}$$

2.2 One-Equation Dynamic Model

One-equation dynamic model (OD) is derived based on the SGS turbulent kinetic energy $k_{sgs} = \frac{1}{2}(\overline{u_k u_k} - \bar{u}_k \bar{u}_k)$ where the production term in the k_{sgs} transport equation is calculated dynamically. The eddy viscosity is calculated based on square root of k_{sgs} which acts as a velocity scale while for the length scale, it is represented by the grid-filter length (commonly computed from the cell volume). The coefficient C_v in Eq. (8) is set to 0.05.

Rewriting the filtered equation of motion (4) and adopting the eddy viscosity assumption yields

$$\frac{\partial \bar{u}_i}{\partial t} + \frac{\partial}{\partial x_j}(\bar{u}_i \bar{u}_j) = -\frac{\partial}{\partial x_i}(\bar{P} + \frac{2}{3}k_{sgs}) + \frac{\partial}{\partial x_j}\left[2(\nu + \nu_t)\bar{D}_{ij}\right], \tag{7}$$

where the SGS eddy viscosity ν_t is expressed as

$$\nu_t = C_v \Delta_v \sqrt{k_{sgs}} \tag{8}$$

and the characteristic length Δ_v is given as [14]

$$\Delta_v = \frac{\bar{\Delta}}{1 + \frac{C_k \bar{\Delta}^2 \bar{D}^2}{k_{sgs}}}. \tag{9}$$

Transport equation which considers the historic effect of k_{sgs} due to the non-equilibrium between production and dissipation has been represented as follows [14,15].

$$\frac{\partial k_{sgs}}{\partial t} + \frac{\partial}{\partial x_j}(\bar{u}_j k_{sgs}) = P_{k_{sgs}} - C_\varepsilon \frac{k_{sgs}^{\frac{3}{2}}}{\bar{\Delta}} - \varepsilon_\omega + \frac{\partial}{\partial x_j}\left[\left(\nu + C_d \Delta_v \sqrt{k_{sgs}}\right)\frac{\partial k_{sgs}}{\partial x_j}\right], \tag{10}$$

The first term in the right-hand side, $P_{k_{sgs}} = -\tau_{ij}\bar{D}_{ij}$, is known as the SGS production term which is responsible for the energy transfer from GS to SGS in the context of the one-equation model. For τ_{ij}, any SGS stress model can be applied. In case of eddy viscosity model of Smagorinsky type, $P_{k_{sgs}}$ in (10) becomes

$$P_{k_{sgs}} = 2(c\bar{\Delta}^2 |\bar{D}|)\bar{D}_{ij}\bar{D}_{ij} = c\bar{\Delta}^2 |\bar{D}|^3. \tag{11}$$

Kajishima and Nomachi [9] applied Germano-Lilly's dynamic procedure [6,7].

$$c = -\frac{1}{2\bar{\Delta}^2}\frac{L_{ij}M_{ij}}{M_{kl}M_{kl}}, \tag{12}$$

where $L_{ij}(= T_{ij} - \tilde{\tau}_{ij}) = \widetilde{\bar{u}_i \bar{u}_j} - \tilde{\bar{u}}_i \tilde{\bar{u}}_j$ and $M_{ij} = \alpha^2 |\tilde{\bar{D}}|\tilde{\bar{D}}_{ij} - \widetilde{|\bar{D}|\bar{D}_{ij}}$.

Dynamic procedure of DSM is used to obtain the coefficient, c. In our work, any smoothing or averaging is not necessary, and thus a negative value of c by Eq. (12) is allowed. The negative value indicates the reverse transfer of energy or from SGS to GS portion and it is important for inhomogeneous cases. It is important to note that the negative value of production term will only

decrease the k_{SGS}. The backscatter of energy is not represented in filtered equation of motion because the eddy viscosity v_t is always positive. Furthermore, the advantage of removing the averaging and smoothing will also make the OD model more flexible for engineering interest in the absence of homogeneous directions. For the energy losses or dissipation, Eq. (8) is used.

The second term in Eq. (10) represents the SGS dissipation term. No modification has been added to the length scale of this term. However, an additional dissipation term ε_ω is introduced to consider near wall turbulence solution [16]. The additional dissipation term ε_ω is calculated as

$$\varepsilon_\omega = 2v \frac{\partial \sqrt{k_{sgs}}}{\partial x_j} \frac{\partial \sqrt{k_{sgs}}}{\partial x_j} . \tag{13}$$

The effects of SGS diffusion is accounted for in the last term of Eq. (10). The constant-coefficient for dissipation term is set as 0.835 as recommended by Okamoto and Shima [14] while some references have said that $C_\varepsilon = 1.05$ yields a good agreement with the direct numerical simulation (DNS) and experimental data [17].

3. Numerical Method

In the present simulation, spatially filtered incompressible Navier-Stokes equations (NSE) are discretized based on finite difference method by using in-house code. The diffusion terms in NSE are discretized by the 2nd order central finite difference while the QUICK method is applied to the convective terms. The QUICK method has an advantage in term of numerical stability for the simulation of high Re number flows and has been proven in study done by Han *et al.,* [18]. For the transport equation of k_{SGS}, the non-linear term is solved based on donor-cell method procedure.

Time marching to solve the viscous and convective terms is based on the explicit Adams-Bashforth method of the 2nd order accuracy. Besides that, this method is also used to solve the time marching in the transport equation of k_{SGS}. The pressure Poisson equation is solved using Successive Over-Relaxation (SOR). The computational time step is set as $3.0 \times 10^{-5} c/U_\infty$ giving the maximum CFL number of around 0.2.

4. Outline of Computational Setup
4.1 Grid Arrangement

Computational conditions used in this simulation corresponds to those experiments conducted at the ONERA F1 wind tunnel where the angle of attack was 13.3°, the Reynolds number based on the chord length C and freestream velocity U_∞ and Re_c $(= \frac{CU_\infty}{v})$ = 2.1×10^6 . In order to observe the effects of the OD model, similar computational setup performed by Dahlstrom and Davidson [4], in terms of grid number, was used. The essential difference between our computational setup and Dahlstrom and Davidson [4] is the method of handling the eddy viscosity in the laminar region, where they used an artificial approach by setting the eddy viscosity to zero in the laminar region. Apart from that, mesh used in their simulation is refined in the transition region to capture the laminar-transition phenomena. In our method, no artificial approaches had been performed and this allowed the checking of the capability of the OD model.

In the x-y plane, the so-called C-grid is generated where ξ coordinate goes around the airfoil and η is in the outward direction from the solid wall and cut-line after the trailing edge. Meanwhile ζ is in the spanwise direction. The domain is extended up to 20C (20 times of the chord length) in both the X-direction and the Y-direction as shown in Figure 2. Table 1 lists the detail of the grid which includes

the mesh resolution in wall units. The spanwise averaged local friction velocity is used to obtain the dimensionless grid resolution $\Delta x^+ = \frac{\triangle x U_\tau}{\nu}$.
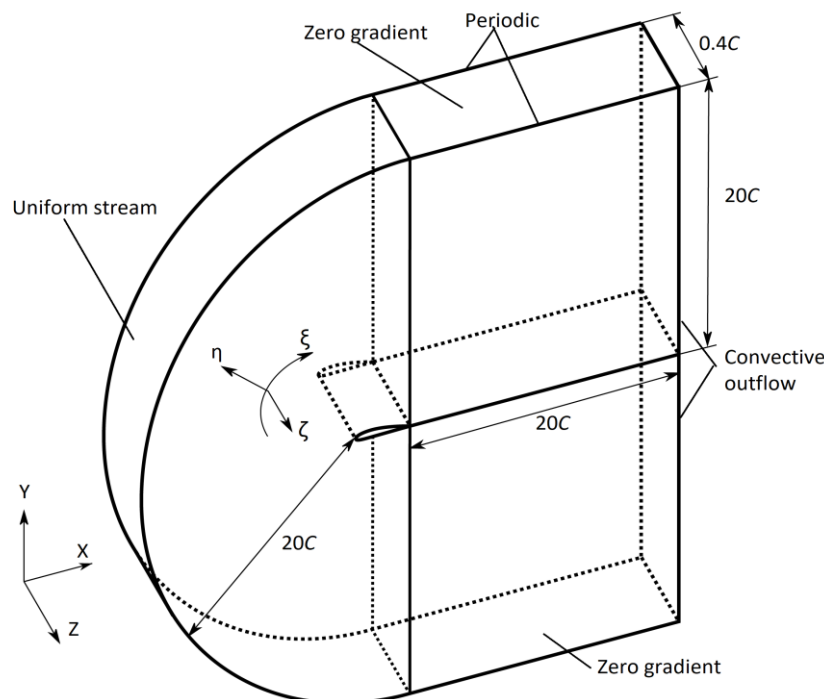

Fig. 2. Computational domain for C-type Grid

Table 1
Detail of grid

$\xi \times \eta \times \zeta$	$720 \times 65 \times 33$
# nodes along the wake (ξ-direction)	151
# nodes on pressure side (ξ-direction)	211
# nodes on suction side (ξ-direction)	211
Cell sizes at leading edge (height)	$5 \times 10^{-5}C$
Cell sizes at trailing edge (height)	$5 \times 10^{-5}C$
$\Delta x^+, \Delta y^+, \Delta z^+$ (wall units)	90~700, 2~14,100~900
Computational domain	$20C \times 20C \times 0.4C$

4.2 Boundary Conditions

The cylindrical surface of the upstream side of the computational domain is set as inlet boundary condition where the freestream velocities U_∞ without turbulence is used. At the top and bottom boundaries, the normal components of the gradients of variables are set to zero. Convective boundary conditions $\frac{\partial \overline{u}_i}{\partial t} + U_\infty \frac{\partial \overline{u}_i}{\partial x} = 0$ is applied as outlet boundary conditions. In addition, no-slip boundary condition is enforced around the airfoil. In spanwise direction, periodic boundary condition is employed. For the pressure boundary conditions, a Neumann boundary condition $\frac{\partial \bar{p}}{\partial n} = 0$ is implemented for inflow, outflow, top and bottom boundaries.

5. Results and Discussion

5.1 Laminar-transition

In our simulation, no ad-hoc method is used as a treatment for laminar-transition region. The subgrid scale kinetic energy k_{SGS} is set to zero at the wall and clipping procedure is implemented for the negative k_{SGS}. This clipping procedure is required to ensure the eddy viscosity v_t in equation of motion is always positive. Based on our experience, the stability of OD model has been proven despite of no averaging in homogeneous direction to calculate the coefficient. The initial data is taken from a fully-developed stage of DSM simulation, where at the first step, the k_{SGS} is calculated via Eq. (8). The statistical data was collected for 9.3-time units (C/U_∞).

Figure 3 displays time and spanwise averaged velocity vectors and instantaneous of k_{SGS} contour plot. The instantaneous of k_{SGS} is plotted as a background to visualize the location of the k_{SGS} development. The velocity vector in Figure 3 displays a thin laminar boundary layer developed around the leading edge. On the other hand, it is obvious that the subgrid scale kinetic energy k_{SGS} started to develop after x/C = 0.11. Results from the ONERA wind tunnel revealed that the thin laminar boundary layer also developed around the leading edge, laminar separation bubble was formed and the flow reattached around x/C =0.12 [4].
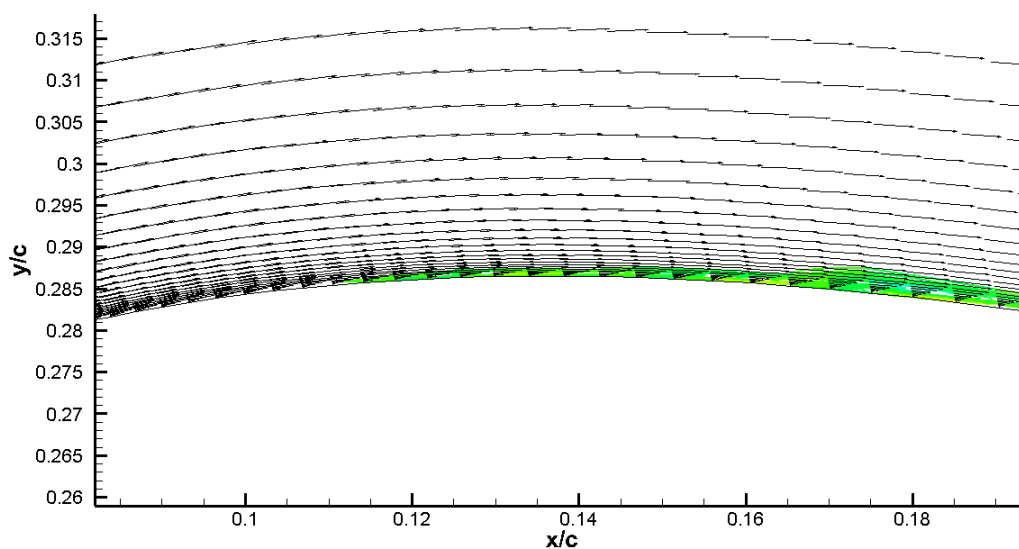

Fig. 3. Averaged velocity vectors around leading edge at slice z/C = 0.2

Figure 4 shows normal components of Reynolds stress around the suction side of the airfoil. The R11 and R22 of the figure legends denote the normal component of Reynolds stress corresponds to the direction parallel and normal to the airfoil wall respectively. While R33 corresponds to the spanwise component. Two graphs are plotted around y/C = 0.0003 and y/C = 0.001. The results, that is without turbulence stress, indicates that the laminar region is successfully captured. This exhibits that the OD model managed to reduce the dependency of fine grid resolution to capture a very thin laminar boundary layer.
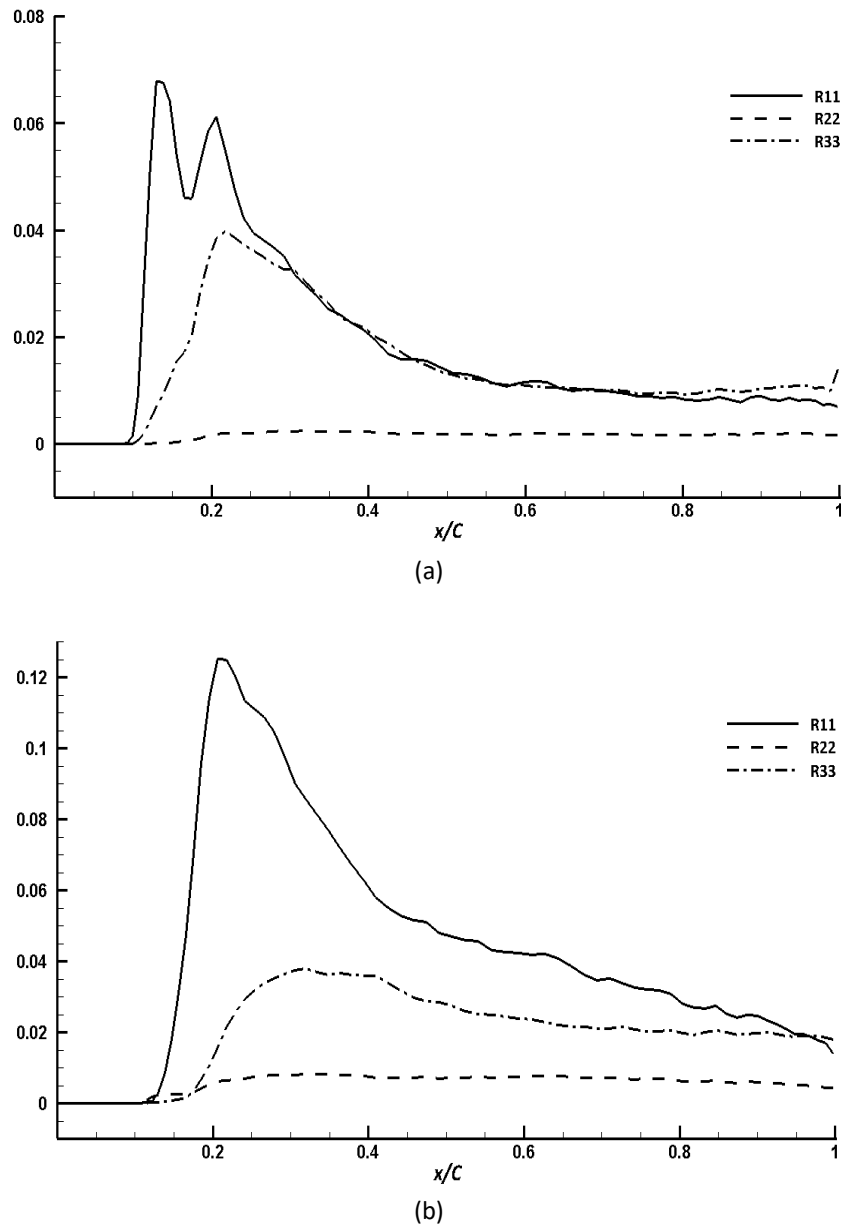
Fig. 4. Normal components of Reynolds stress at (a) y/C = 0.0003 and (b) y/C = 0.001

5.2 Pressure Coefficient and Skin Friction Coefficient

Profile of mean pressure coefficient $C_P = 2(p - p_\infty)/\rho U_\infty^2$ and skin friction coefficient $C_f = 2\tau_\omega/\rho U_\infty^2$ (τ_ω represents the wall shear stress) are plotted in Figure 5. In the LESFOIL project, plot of C_p and C_f are very important to justify the existence of laminar separation bubble around the leading edge and trailing edge separation [3,4,19]. For the simulation, this phenomenon is commonly described by looking at the plateau of C_p plot and negative value of skin friction coefficient C_f. Unfortunately, this phenomenon cannot be captured by the OD model where no plateau is observed around the leading edge and the C_f plot also displays a positive value around this region.

For the skin-friction coefficient C_f, the wall shear stress is defined as $\tau_\omega = \mu \left(\frac{\partial u_b}{\partial n}\right)_{n=0}$ where u_b is the velocity component along the airfoil surface. The result for the OD model is not identical to the experimental data. Insufficient resolution for streamwise and spanwise direction is found to be one

of the reasons for underprediction of skin-friction coefficient. As a consequence, development of turbulent structures is not accurately represented when the resolution does not reached the required mesh resolution [2]. In addition, friction velocity is most influenced by the spanwise resolution, Δz^+ as pointed out by Rezaeiravesh and Liefvendahl [20].
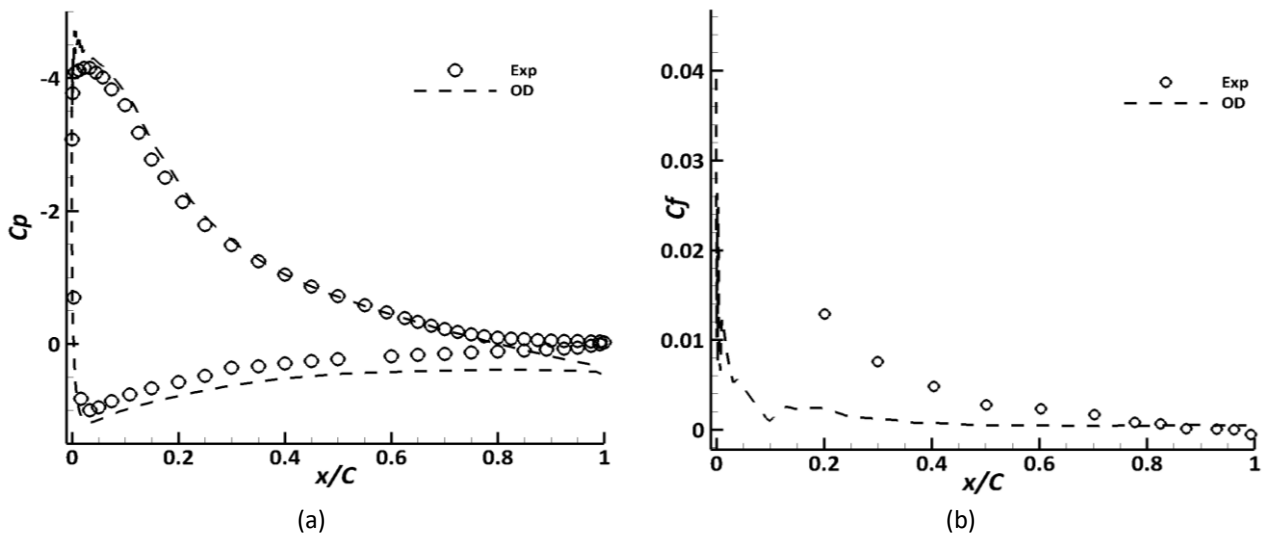

Fig. 5. Averaged (a) pressure coefficient C_p and (b) friction coefficient C_f

5.3 Total Turbulent Kinetic Energy

Total turbulent kinetic energy is defined as a summation of subgrid scale turbulent kinetic energy k_{SGS} and grid scale turbulent kinetic energy, $k_{GS} = \frac{u'^2 + v'^2 + w'^2}{2}$. In the OD model, the production term $-\tau_{ij}\overline{D}_{ij}$ is described differently from other dynamic versions of one-equation model. Figure 6 shows the k_t and k_{SGS} plotted at the location of y/C =0.0003 and y/C = 0.001. From these plots, it can be seen that the dynamic procedure implemented in the production term manage to identify non-turbulent region around the leading edge. In contrast to conventional eddy viscosity model where SGS eddy viscosity v_t is exist due to the velocity gradient even in the laminar region. Furthermore, at y/C = 0.0003, the first peaks for k_t and k_{SGS} are identical to each other at approximately x/C = 0.13. This peak is possibly associated with the location of flow reattachment phenomena. This peak is also identical to the normal component of Reynolds stress (Figure 4), where flow from laminar region (no resolved stresses) reached the peak as the flow reattached. This also indicates the beginning of the development of turbulent boundary layer. A similar trend is observed for both locations except for the peak of kinetic energy. Therefore, the OD model had resolved the issue to remove the turbulent kinetic energy and eddy viscosity in the laminar region without any artificial methods and grid refinement.

Dynamic procedure implemented for the OD model reveals that the total kinetic energy remains zero in the laminar region and switches to some finite value in the transition to turbulent region. In the OD model, the dynamic procedure was applied to determine the coefficient in the production term of turbulent kinetic energy equation k_{SGS}. As described in section 2.2, dynamic procedure to evaluate the coefficient in production term can become negative, and as consequences will lead to a decrease of k_{SGS}. The advantage of applying the eddy viscosity model of Smagorinsky type in production term is proven in this study where no self-reproduction of k_{SGS} in the laminar region as highlighted by Inagaki and Abe [12] and Davidson [13]. The clipping of k_{SGS} has also leads other terms

in transport equation of k_{SGS} become zero in laminar region. On the other hand, the terms in k_{SGS} transport equation should balance in the turbulent region especially in the vicinity of the wall.
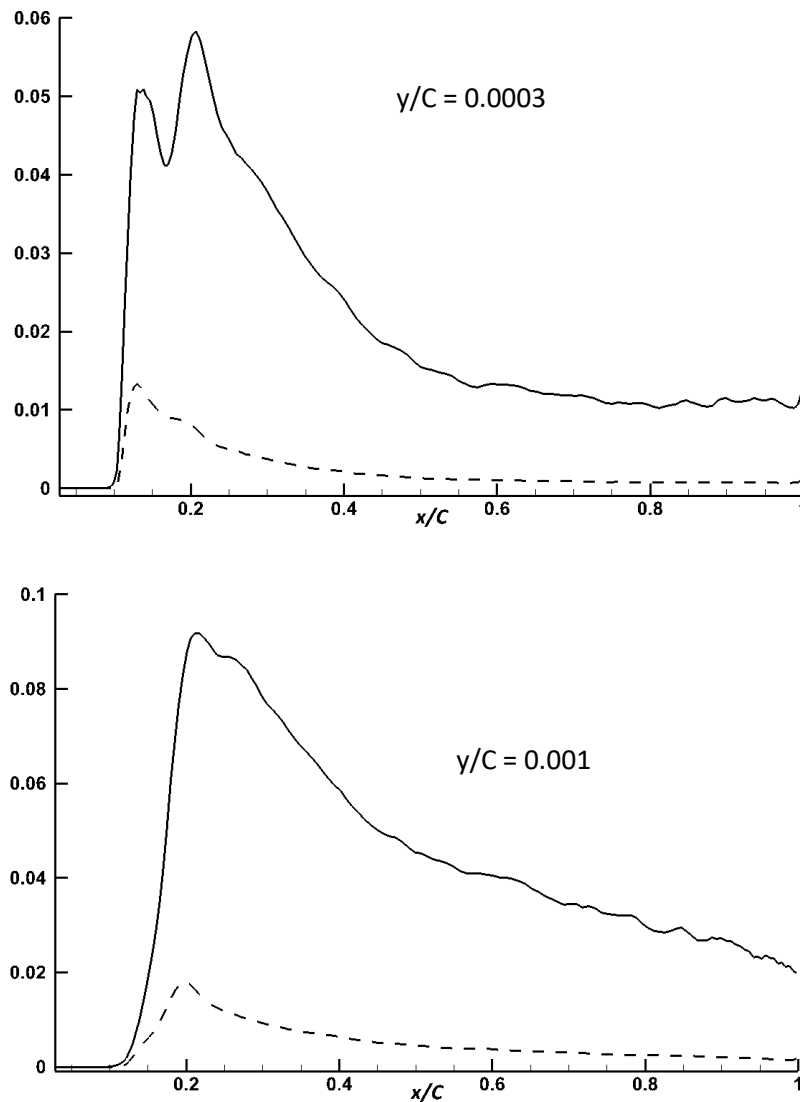

Fig. 6. Averaged total turbulent kinetic energy (k_t)-solid line and SGS kinetic energy (k_{SGS})-dashed around suction side of the airfoil. Vertical axis is k/U_∞^2

In order to ensure the balance of terms in k_{SGS} equation, the averaged of production, convection, diffusion and dissipation terms in the transport equations of k_{SGS} or budget of SGS kinetic energy was plotted in Figure 7. This figure is plotted at the location of $x/C = 0.12$ which indicates the laminar-transition region. It is obvious that the terms in energy budget is relatively important in the vicinity of the wall. The transport equation for k_{SGS} based on the OD model reveals that the production term is balanced with the summation of dissipation and convection term. On the other hand, the diffusion and dissipation from molecular viscosity and additional dissipation term (see Eq. (13)) respectively are almost in balance on the wall. In the OD model, the dissipation term is defined as a summation of SGS dissipation term and the additional dissipation term (terms 2 and 3 in Eq. (10)). Hence, the additional dissipation term of Eq. (13) is important for the OD model in the vicinity of the wall.
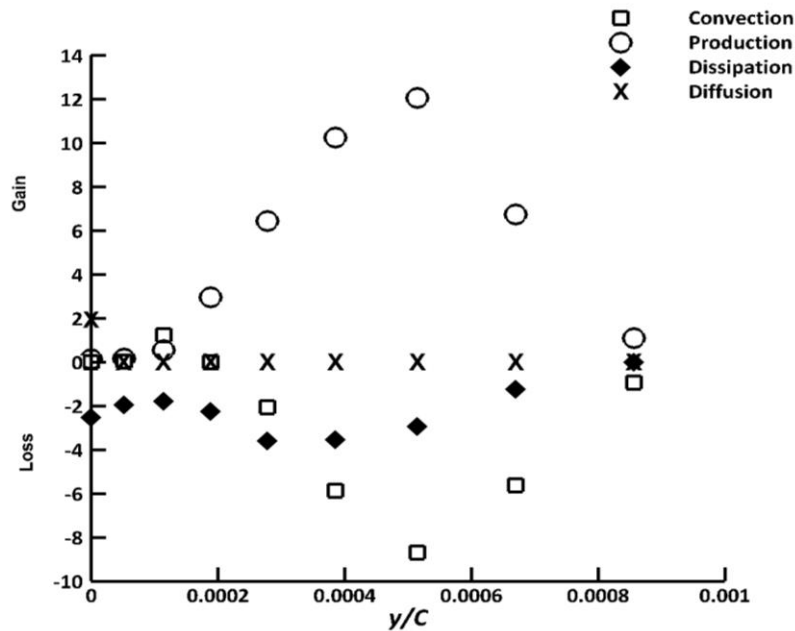
Fig. 7. Budget of SGS kinetic energy at *x/C* = 0.12

6. Conclusions

The OD model is used to predict a complex flow around A-airfoil at higher Reynolds number and near-stall condition. The advantage of the OD model to capture the switching of kinetic energy between laminar and transition flow around an airfoil is proven in this study based on k_{SGS} budget analysis. Meanwhile, the dynamically-determined production term based on the eddy viscosity model of Smagorinsky type in k_{SGS} transport equation also proved to be the best representation for the energy transfer between GS to SGS components. Our visualization of k_{SGS} also confirmed that the SGS energy automatically turned to zero in the laminar region and the laminar-to-transition point observed agreed considerably well with the experimental data, thus verifying a desirable feature of OD for complex flow phenomenon.

In addition, the OD model performed well with coarser grid resolution in capturing the laminar and transition regions. However, this coarse grid resolution is found to be unable to predict the turbulent structure and as a result the trailing edge separation also could not be reproduced. Therefore, the anisotropic SGS model that can cope with a low grid dependency as highlighted by Inagaki and Abe [12] should be considered in our future work.

In terms of numerical method, any smoothing or averaging in homogeneous direction is not necessary. Even in the region where the dynamic procedure gave a negative value for production rate of SGS kinetic energy, it only decreases the total value of k_{SGS} without any effect on the numerical stability. Besides that, the OD model also could be considered as a simple model where any parameters such as distance to the wall and damping function are not required. Hence, we believe this OD model is an encouraging SGS model which is capable of dealing with a variety of real engineering applications and its robustness is very promising for dynamic stall analysis of the airfoil.

References

[1] Davidson, Lars, Davor Cokljat, Jochen Fröhlich, Michael A. Leschziner, Chris Mellen, and Wolfgang Rodi, eds. *LESFOIL: Large Eddy Simulation of Flow Around a High Lift Airfoil: Results of the Project LESFOIL Supported by the European Union 1998–2001*. Vol. 83. Springer Science & Business Media, 2012.

[2] Mary, Ivan, and Pierre Sagaut. "Large eddy simulation of flow around an airfoil near stall." *AIAA journal* 40, no. 6 (2002): 1139-1145.

[3] Asada, Kengo, and Soshi Kawai. "Revisiting LESFOIL: Wall-resolved LES of Flow Around an Airfoil at Re_c= 2.1× 10^6." In *2018 AIAA Aerospace Sciences Meeting*, p. 0840. 2018.

[4] Dahlstrom, S., and Lars Davidson. "Large eddy simulation of the flow around an airfoil." In *39th Aerospace Sciences Meeting and Exhibit*, p. 425. 2001.

[5] Dahlström, Simon, and Lars Davidson. "Large eddy simulation applied to a high-Reynolds flow around an airfoil close to stall." In *41st Aerospace Sciences Meeting and Exhibit*, p. 776. 2003.

[6] Germano, Massimo, Ugo Piomelli, Parviz Moin, and William H. Cabot. "A dynamic subgrid-scale eddy viscosity model." *Physics of Fluids A: Fluid Dynamics* 3, no. 7 (1991): 1760-1765.

[7] Lilly, Douglas K. "A proposed modification of the Germano subgrid-scale closure method." *Physics of Fluids A: Fluid Dynamics* 4, no. 3 (1992): 633-635.

[8] Ghosal, Sandip, Thomas S. Lund, Parviz Moin, and Knut Akselvoll. "A dynamic localization model for large-eddy simulation of turbulent flows." *Journal of fluid mechanics* 286 (1995): 229-255.

[9] Kajishima, Takeo, and Takayuki Nomachi. "One-equation subgrid scale model using dynamic procedure for the energy production." *Journal of Applied mechanics* 73, no. 3 (2006): 368-373.

[10] Taghinia, Javad, and Md Mizanur Rahman. "Large eddy simulation of round impinging jet with one-equation subgrid scale model." *International Journal of Heat and Mass Transfer* 116 (2018): 1250-1259.

[11] Taghinia, Javad, Md Mizanur Rahman, Timo Siikonen, and Ramesh K. Agarwal. "One-equation sub-grid scale model with variable eddy-viscosity coefficient." *Computers & Fluids* 107 (2015): 155-164.

[12] Inagaki, Masahide, and Ken-ichi Abe. "An improved anisotropy-resolving subgrid-scale model for flows in laminar–turbulent transition region." *International Journal of Heat and Fluid Flow* 64 (2017): 137-152.

[13] Davidson, Lars. "LES of recirculating flow without any homogeneous direction- A dynamic one-equation subgrid model." *Turbulence, heat and mass transfer* 2 (1997): 481-490.

[14] Okamoto, Masayoshi, and Nobuyuki Shima. "Investigation for the One-Eaquation-Type Subgrid Model with Eddy-Viscosity Expression Including the Shear-Damping Effect." *JSME International Journal Series B Fluids and Thermal Engineering* 42, no. 2 (1999): 154-161.

[15] Yoshizawa, Akira, and Kiyosi Horiuti. "A statistically-derived subgrid-scale kinetic energy model for the large-eddy simulation of turbulent flows." *Journal of the Physical Society of Japan* 54, no. 8 (1985): 2834-2839.

[16] Jones, W. P., and Brian Edward Launder. "The prediction of laminarization with a two-equation model of turbulence." *International journal of heat and mass transfer* 15, no. 2 (1972): 301-314.

[17] Taghinia, Javad. "Sub-grid Scale Modeling in Large Eddy Simulation with Variable Eddy-Viscosity Coefficient." (2015).

[18] Han, Changhwa, and Takeo Kajishima. "Large eddy simulation of weakly compressible turbulent flows around an airfoil." *Journal of Fluid Science and Technology* 9, no. 4 (2014): JFST0063-JFST0063.

[19] Kawai, Soshi, and Kengo Asada. "Wall-modeled large-eddy simulation of high Reynolds number flow around an airfoil near stall condition." *Computers & Fluids* 85 (2013): 105-113.

[20] Rezaeiravesh, Saleh, and Mattias Liefvendahl. "Effect of grid resolution on large eddy simulation of wall-bounded turbulence." *Physics of Fluids* 30, no. 5 (2018): 055106.